Available online at www.sciencedirect.com

ScienceDirect

Geochimica et Cosmochimica Acta 71 (2007) 2158–2169

Geochimica et Cosmochimica Acta

www.elsevier.com/locate/gca

Studies of Cd(II)–sulfate interactions at the goethite–water interface by ATR-FTIR spectroscopy

G.Y. Zhang [a], D. Peak [b,*]

[a] Department of Resources and Environmental Sciences, Agricultural University of Hebei, Baoding 071001, PR China
[b] Department of Soil Science, University of Saskatchewan, 57 Campus Drive, Saskatoon, SK, S7N 5A8, Canada

Received 16 May 2006; accepted in revised form 20 December 2006; available online 26 January 2007

Abstract

A combination of macroscopic experiments and *in situ* attenuated total reflectance Fourier transform infrared (ATR-FTIR) spectroscopy was used to study Cd(II)–sulfate interactions on the goethite–water interface. The presence of SO_4 dramatically promoted Cd adsorption at lower pH (pH 5.5–6.5) and had a smaller effect at higher pH. ATR-FTIR studies indicated sulfate adsorption on goethite occurred via both outer- and inner-sphere complexation. The relative importance of both complexes was a function of pH and sulfate concentration. ATR-FTIR spectra provided direct evidence of the formation of Cd–SO_4 ternary surface complexes on goethite. In addition to ternary complexes, Cd specifically sorbed on goethite promoted SO_4 adsorption via changing the surface charge, and caused additional SO_4 adsorption as both inner- and outer-sphere complexes. The relative importance of ternary complexes versus electrostatic effects depended upon pH values and Cd concentration. Ternary complex formation was promoted by low pH and high Cd levels, whereas electrostatic effects were more pronounced at high pH and low Cd levels. A portion of SO_4 initially sorbed in inner-sphere complexes in the absence of Cd was transformed into Cd–SO_4 ternary complexes with increased Cd concentration.

1. INTRODUCTION

Numerous macroscopic studies have shown that oxyanions can substantially affect sorption of metals on mineral surfaces (Benjamin and Leckie, 1982; Marcano-Martinez and McBride, 1989; Ali and Dzombak, 1996; Bargar et al., 1998; Ostergren et al., 2000; Swedlund et al., 2003; Lackovic et al., 2004). The formation of stable metal–oxyanion aqueous complexes and competition between metal cations and the anions for the same surface sites may reduce metal adsorption in the presence of anions (Benjamin and Leckie, 1982; Theis and West, 1986). Alternatively, the presence and co-adsorption of an anion may increase metal adsorption by formation of ternary complexes, surface precipitation, and electrostatic effects (Lamy et al., 1991; Hoins et al., 1993; Davis and Bhatnagar, 1995; Coughlin and Stone, 1995; Nowak and Sigg, 1996). It is noteworthy that retention of both heavy metals such as Cd, As, Pb and Zn and sulfate were simultaneously enhanced by co-adsorption in ternary systems (Hoins et al., 1993; Ali and Dzombak, 1996; Webster et al., 1998).

It is important to realize that macroscopic experiments can not conclusively determine the sorption mechanisms. Further spectroscopic investigations are beneficial to understanding of the actual reaction mechanisms. Fourier transform infrared (FTIR) spectroscopy is one technique with the ability to characterize the surface complexes of oxyanions on iron oxides in the presence and absence of transition metals. Attenuated total reflectance Fourier transform infrared (ATR-FTIR) spectroscopy is one of the few *in situ* techniques currently available to explore solid/liquid interfacial phenomena. ATR-FTIR provides a viable means of probing the solid/liquid interface without altering the surface characteristics of the sample (Hind et al., 2001).

There have been several studies of metal–sulfate interactions using spectroscopic techniques. Elzinga and

---

* Corresponding author. Fax: +1 306 966 6881.
E-mail address: derek.peak@usask.ca (D. Peak).

0016-7037/$ - see front matter © 2007 Published by Elsevier Ltd.
doi:10.1016/j.gca.2006.12.020

co-workers (2001) conducted studies on Pb(II)–sulfate interactions at the goethite–water interface using a combination of *in situ* ATR-FTIR and Pb L(III) Edge EXAFS spectroscopy. Their results indicated that formation of Pb–SO_4 ternary complexes occurred on goethite surface, and that adsorption of Pb also promoted SO_4 sorption and led to additional formation of inner- and outer-sphere complexes not directly coordinated with Pb. Using the same techniques, Ostergren et al. (2000) had previously studied the co-adsorption of SO_4 and Pb to goethite on molecular scale. They found evidence for the formation of Fe–Pb–SO_4 ternary complexes at the goethite surface, with Pb increasingly sorbed via ternary complex formation as the SO_4 concentration was raised. The results of previous Cd–SO_4–goethite research are in contrast to these two Pb studies. In a Cd EXAFS study, it was reported that enhancement of Cd adsorption on goethite in the presence of sulfate and phosphate is solely due to electrostatic effects and no ternary complexes are observed (Collins et al., 1999). However, it is possible that weaker interactions such as those proposed by previous researchers for Pb would remain unobserved by the Cd EXAFS.study of Collins et al. (1999). EXAFS analysis for Pb in ternary-complex systems was sensitive to changes in the corner- to edge-sharing ratio of metal complexes, and only a single broad Cd–Fe interatomic distance was fit by Collins and coworkers. This average value may not be sensitive to subtle transitions upon ternary complex formation. The ATR-FTIR studies of SO_4 bonding were crucial in ternary complex identification for both Pb–SO_4 studies but were not undertaken by Collins and co-workers.

We hypothesize that many of the changes observed in the Pb–SO_4–goethite system will also occur with Cd. The objective of this research was to investigate how cadmium affects co-adsorption of sulfate on goethite using a combination of macroscopic methods and *in situ* ATR-FTIR spectroscopy. Specifically, the study is to elucidate the effects of Cd concentration, pH values and sulfate concentration on the mechanisms of Cd–SO_4 interactions on goethite surface.

1.1. Infrared theory

The relationship between the symmetry of sulfate complexes and their infrared spectra is well established (Persson and Lovgren, 1996; Hug, 1997; Peak et al., 1999, 2001; Lefevre, 2004), and it is possible to assign molecular symmetry based on the number and position of peaks that appear in the mid-infrared region, Under aqueous conditions, there are two infrared sulfate vibrations that are accessible to spectroscopic investigation. They are the nondegenerate symmetric stretching ν_1 and the triply degenerate asymmetric stretching ν_3 bands (Persson and Lovgren, 1996). The relationship between the symmetry of surface complexes and their resulting infrared spectrum is summarized in Fig. 1.

More recently, the above classical interpretation of sulfate IR spectra has been somewhat modified by S K-Edge XAS (Majzlan and Myneni, 2005) and theoretical calculations (Paul et al., 2005). Majzlan and Myneni (2005) studied the speciation of ferrous and ferric iron and sulfate in acidic solutions with both ATR-FTIR and S K-Edge XANES spectroscopy. They concluded that inner-sphere monodentate complexation between Fe(III) and sulfate did occur in samples, but that it was a minor (~10%) component whereas the bulk of the interactions corresponded to hydrogen bonding interactions. They extrapolated this behavior to sulfate adsorption on Fe(III) oxide surfaces because the ATR-FTIR spectra of aqueous Fe(III)–SO_4 complexes at pH 2 was similar to previously reported SO_4–goethite data from a variety of references discussed previously. Their overall conclusion was that H-bonding is the dominant adsorption mechanism between sulfate and iron oxides. This does seem reasonable, but it is not completely consistent with SeO_4/goethite EXAFS studies (Peak and Sparks, 2002), which have shown that inner-sphere surface com-

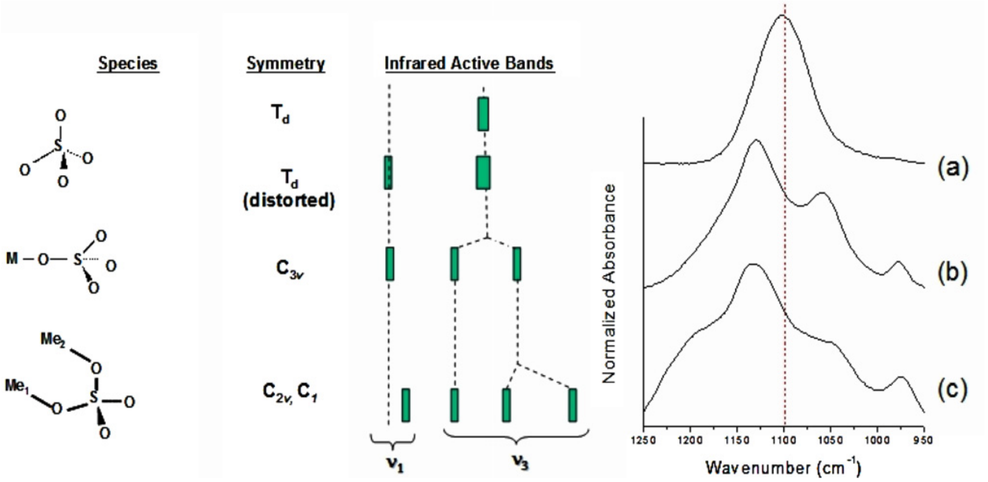

Fig. 1. The relationship between the molecular symmetry of sulfate complexes and the observed infrared spectrum they produce. (a) ATR-FTIR spectrum of 100 mM aqueous sulfate (b) ATR-FTIR spectrum of 25 μM sulfate adsorbed on hematite at pH 4.0 (c) Transmission-mode spectrum of schwertmannite, a poorly crystalline iron(III) oxy-hydroxy-sulfate mineral.

plexes will form at low pH on the goethite surface. The chemical properties of SeO_4 and SO_4 are both very similar, and so similar bonding mechanisms are expected to occur with both oxyanions.

Another observation that Majzlan and Myneni made about the FTIR results was that using ferric nitrate vs. chloride salts for the solutions had no effect on the resulting solution spectra. This is unexpected, as a speciation program (Mineql+) predicts a dramatically different amount of $FeSO_4^+$ in the presence of Cl- (~25% of total SO_4) and nitrate (~95% of total SO_4) for pH 2.0. One could interpret this to mean that the ATR-FTIR spectral features of $FeSO_4^+$ and other possible mixtures of bisulfate/hydrogen-bonded SO_4 species may not be unique, and that symmetry rules and splitting are simply not conclusive for sulfate species adsorbed on iron oxide surfaces.

The nature of sulfate surface complexes on hematite was also investigated by Paul and co-workers (2005) using computational chemistry. They concluded that the major bonding mechanism of sulfate on hematite was bidentate binuclear inner-sphere, and that upon dehydration a conversion to bidentate bisulfate complexes occurred. They predicted that a hydrogen-bonded sulfate would have a similar number of peaks as the bidentate binuclear species, but the positions of the peaks were further from the experimental values and so the inner-sphere complex was more likely. Their H-bonded sulfate is different from the assignment of Majzlan and Myneni (2005) in that it is bidentate in its coordination to iron waters of hydration rather than monodentate. Their analysis of the peaks obtained from sulfate adsorbed on goethite was that a bidentate binuclear complex with peaks occurring in different positions from hematite would best describe the inner-sphere complexes on goethite. It is unclear from their paper why the bidentate binuclear complexes would produce different positions and far different relative intensities on the two different sorbent phases.

When the above findings are considered together, a large portion of the apparent contradictions in the literature can be resolved. First of all, XAS results seem to predict a small amount of inner-sphere complexation while the inner-sphere peaks are much more pronounced in ATR-FTIR studies. This discrepancy could be simply due to differences in molar absorptivity coefficients between the inner-sphere and outer-sphere complexes. If the absorptivity coefficient for the inner-sphere peaks is larger than the outer-sphere ones, then the importance of inner-sphere complexes would be exaggerated in FTIR experiments. Second, one of the major conclusions of both the XAS and computational studies is that hydrogen bonding is another type of potential interaction of sulfate on iron oxide surfaces that may distort spectra of sulfate. If that is the case, then both inner-sphere monodentate sulfate and hydrogen bonded sulfate may be considered together as responsible for the 1170, 1132, and 1050 cm^{-1} "inner-sphere" peaks of previous studies. In any case, the general description of "inner-sphere" vs. "outer-sphere complex formation is probably better framed in terms of strongly coordinated (inner-sphere), intermediately coordinated (hydrogen bonded), and weakly coordinated (outer-sphere sulfate in the diffuse layer).

The above interpretation is also consistent with results from employing an extended triple layer model (ETLM) to describe adsorption of sulfate on goethite (Fukushi and Sverjensky, 2007). The ETLM was specifically developed "developed to help integrate published experimental spectroscopic and theoretical molecular evidence of the identity of oxyanion surface species with a surface complexation model of adsorption." (Fukushi and Sverjensky, 2007). The ETLM found that a mixture of an inner-sphere monodentate complex and an outer-sphere (or H-bonded) complex provided the best description of the data.

2. MATERIALS AND METHODS

2.1. Goethite synthesis

The goethite was synthesized using the method of Schwertmann et al. (1985). The synthesis was conducted inside a glovebox under a N_2 atmosphere. Initially, ferrihydrite was precipitated by adding 50 ml of 1 M ferric nitrate solution to 450 ml of 1 M KOH. This suspension of amorphous hydrous ferric oxide was then aged for 14 days at 25 °C. The suspension was next washed using distilled-deionized (DDI) water (18.2 MΩ, Barnstead NanoPure) to remove residual KOH via centrifugation. The rinsed solid was then resuspended in 0.4 M HCl and shaken for 2 h using a mechanical shaker. This treatment was used to remove any remaining ferrihydrite from the surface of the goethite. The acidified goethite suspension was again washed via centrifugation to remove both HCl and dissolved iron. Finally, the goethite was freeze-dried. The external surface area determined from N_2 BET was 73.86 m^2/g and the point of zero salt effect was 8.4, as determined via potentiometric titration in 0.1, 0.01, and 0.001 M KNO_3.

2.2. Macroscopic methods

Solutions were prepared from AR (or GR) grade chemicals and 18.2 MΩ, DDI water. The experiments were all conducted under the conditions of room temperature (25 ± 1 °C), solid to liquid ratio of 1:1000 and 0.01 M $NaNO_3$ as background electrolyte

2.2.1. *Adsorption isotherms*

Adsorption isotherms of Cd on goethite were performed by adding goethite suspension, 0.01 M $NaNO_3$ as background electrolyte, and the desired concentration of Cd (10–350 μM) from a stock solution of $Cd(NO_3)_2$. The pH of these suspensions was next adjusted to 6.00 ± 0.02 by adding small volumes of dilute HNO_3 or NaOH. Then all samples were shaken for 24 h with regular pH adjustments to maintain a constant pH of 6 during the adsorption reaction. After 24 h, the suspension samples were centrifuged at 3000 rpm and supernatants were collected. All supernatants were filtered by using 0.1 μm filter paper and the Cd content in the supernatant solution was determined by FAAS (flame atomic absorption spectroscopy). The effect of 1 mM sulfate on Cd adsorption isotherm at pH 6 was conducted using similar procedures. Initially, the goethite suspension, background electrolyte and sulfate (Na_2SO_4)

were added into tubes. The pH of suspensions was adjusted to required pH value by using dilute HNO_3 and NaOH and then shaken for 24 h to allow for sulfate adsorption to complete. Then $Cd(NO_3)_2$ was added and all subsequent procedures were the same as the above Cd adsorption isotherm.

Sulfate adsorption isotherms were also performed at pH 4 and 6 based on the conditions above. The initial concentration of sulfate was set up in the range of 30–800 μM.

2.2.2. pH adsorption edges

Initially, a suspension of goethite, background electrolyte and sulfate (0, 400 and 800 μM, respectively) prepared in a 100 ml reaction vessel and adjusted to about 3.5 using $HNO_{3.}$ Then the desired volume of $Cd(NO_3)_2$ stock solution was added to reach a final concentration of 100 μM Cd. A computerized titration system (Methrohm) was utilized to add 0.1 M NaOH into the suspension and adjust pH from 3.5 to 10 in 1 pH unit steps. During the experiments, continuous N_2-gas sparging and stirring (via a magnetic stir bar) were employed. After achieving each pH endpoint, 10 mL samples were pipetted into centrifuge tubes. The tubes were then shaken for 24 h. Final equilibrium pH of suspensions were measured and then the suspensions were centrifuged, supernatants were filtered and Cd content in final supernatants was determined by FAAS.

2.3. In situ ATR-FTIR spectroscopy

All FTIR experiments were conducted using a BRUKER-EQUINOX 55 FTIR equipped with a purge gas generator and a MCT detector. A multibounce horizontal ATR accessory and flow cell (Pike Technologies) were used for sampling. Spectra were the result of 1000 co-added scans at a resolution of 4 cm^{-1} unless otherwise noted. A thin goethite film was adhered to the 45° ZnSe ATR crystal by allowing 8 drops of 0.01 M NaCl (at a pH 4) and 4 drops of a 20 g/L goethite slurry. This suspension was then mixed and spread evenly across the surface of the crystal using the pipette tip and allowed to dry. After drying, the film was rinsed at least two times with 0.01 M NaCl. Rinsing removes any particles that are loosely deposited and are more likely to erode during the experiment. The rinsed and air-dried ATR crystal air was then placed into the flow cell, and then onto the horizontal ATR sample stage. The flow cell was finally connected to a reaction vessel containing 1 L of 0.01 M $NaNO_3$ background electrolyte. $NaNO_3$ was used due to its very low complexation constant with cadmium. Our preliminary studies demonstrated that the N–O vibrations would not interfere with any of the S–O vibrations of interest for our experiments, and data analysis was not an issue in the 1250–950 cm^{-1} range in any of our experiments. The vessel was N_2 gas purged and pH controlled. To start the experiment, the background electrolyte was passed through the flow cell at a flow rate of 1 mL/min. A background spectrum consisting of the absorbance of the ZnSe crystal, background electrolyte solution, and the goethite deposit was collected every 10 min. Generally, after 2–3 h, there was no difference between successive background spectra, which indicated that the goethite deposit had equilibrated with the background electrolyte. At this time, the final background spectrum was collected and an adsorption experiment was started by introducing reactants (sulfate, cadmium, or both) into the reaction vessel. All successive spectra were collected as a ratio to the background spectrum.

2.3.1. Sulfate pH adsorption/desorption envelopes

One potential experimental method to differentiate H-bonding and inner-sphere complexation between sulfate and goethite using ATR-FTIR is to conduct adsorption/desorption studies by first decreasing pH to adsorb sulfate and then returning the pH to its original value and monitoring the change in surface complexes.

2.3.2. Adsorption isotherm experiments

For adsorption isotherm experiments, equilibrium was defined as the point where no further increase in the infrared spectra arising from adsorbed sulfate was observed over a ten minute period. The adequate amount of stock solution 0.1 M Na_2SO_4 or $Cd(NO_3)_3$ needed to adjust the remaining volume to the appropriate concentration was calculated from the flow rate (1 ml min^{-1}) and the time elapsed since the pump was started. This amount of reactant was then added to the reaction vessel and the system allowed to reach a new equilibrium.

2.3.3. Effect of Cd level on sulfate adsorption to goethite

For these experiments the goethite deposit on the ZnSe crystal was first equilibrated with 25 μM Na_2SO_4 solution. Then Cd was added to the reaction vessel connected to the flow cell. The addition of Cd to the system increased successively with Cd concentration of 10, 25, 50, 100 and 500 μM. For each level of Cd in solution, the sulfate adsorption on goethite deposit was monitored till there was no further increase in spectra of sorbed sulfate with time.

2.3.4. Sulfate FTIR standards

Additionally, a number of spectra of aqueous SO_4 standards were obtained. These were, 100 mM Na_2SO_4, 50 mM H_2SO_4, and a $CdSO_{4(aq)}$ complex obtained by combining 100 mM Na_2SO_4 and 1 M $Cd(NO_3)_2$. Speciation calculations in MINEQL1 indicated that 95% of total SO_4 was present as ${CdSO_{4(aq)}}^0$ complex in our standard. The presented aqueous spectra are the result of subtracting a reference spectrum of either DDI water or 1 M $Cd(NO_3)_2$ from the SO_4 standard to produce a spectrum of only the SO_4 compound. A sample of precipitated solid cadmium sulfate hydroxide hydrate precipitate, $CdSO_4{\cdot}3.5Cd(OH)_2(H_2O)_n$ was also prepared by mixing 60 mL of 0.1 M Na_2SO_4 and 20 mL of 0.3 M $Cd(NO_3)_2$ with drop-wise addition of 2 M NaOH until precipitation occurred. The resulting white precipitate was separated via vacuum filtration and washed three times with DDI water (Collins et al., 1999). A suspension of the solid was made using DDI water, air-dried onto the ATR crystal, and then the spectrum of $CdSO_4{\cdot}3.5Cd(OH)_2(H_2O)_n$. was measured.

3. RESULTS

3.1. Macroscopic experiments

Fig. 2 shows the results of an adsorption isotherm of Cd on goethite at pH 6 in both the absence and presence of 1 mM sulfate. At 100 μM initial Cd, the amount of Cd adsorption in the presence of 1 mM SO_4 was nearly three times that of the sulfate-free system (17.09 vs. 49.43 mmol/kg, respectively). Both Cd isotherms were described well with the Langmuir equation. The maximum adsorption amounts were 69.74 and 25.29 mmol/kg and correlation coefficients were (at 95% confidence limits) 0.9819 and 0.9558, respectively. These results indicated that sulfate markedly promoted Cd adsorption on goethite at pH 6.

A comparison of sulfate adsorption isotherms on goethite at pH 4 and 6 are shown in Fig. 3. Both sulfate isotherms can also be fit using the Langmuir equation with maximum adsorption amounts of 138.4 and 35.08 mM/kg, with respective correlation coefficients (at 95% confidence limits) of 0.9723 and 0.8973. The maximum amount of sulfate adsorbed on goethite at pH 4 was approximately three times greater than that at pH 6. These results demonstrate that sulfate adsorption on goethite is more favorable at decreased pH.

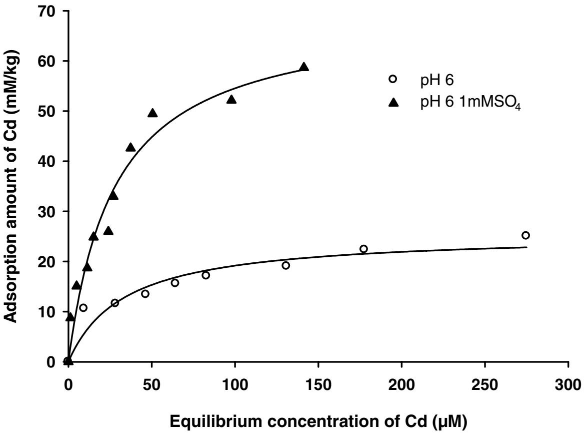

Fig. 2. Adsorption isotherm of Cd on goethite at pH 6.

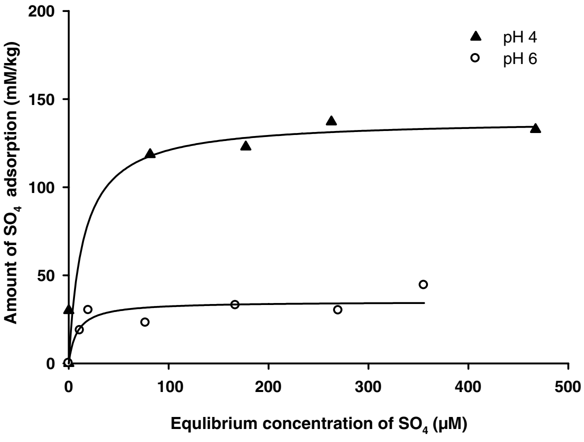

Fig. 3. Adsorption isotherm of sulfate on goethite at pH 4 and 6.

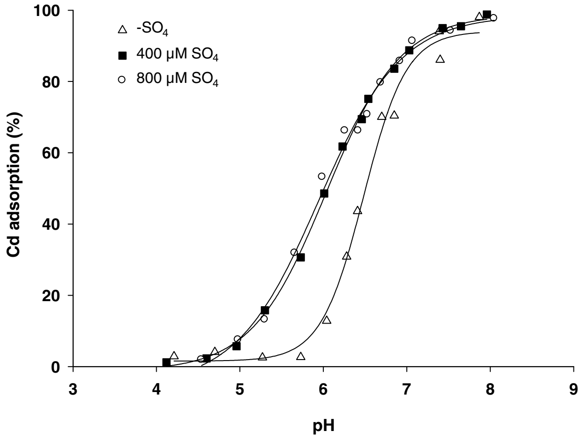

Fig. 4. Effect of pH and sulfate on Cd adsorption on goethite.

Fig. 4 shows pH adsorption edges for Cd in the presence of 0, 400, and 800 μM SO_4. The pH of the cadmium adsorption edge is shifted to lower pH in the presence of sulfate by approximately 0.5 pH units. Between pH 5.5 and 6.5, additional Cd adsorption was dramatically enhanced by introducing sulfate. However, while this obvious difference of Cd adsorption between the absence and presence of sulfate occurred, no clear variations were shown by adding 400 versus 800 μM sulfate in ternary goethite/Cd/SO_4 system.

3.2. In situ ATR-FTIR data

3.2.1. *Adsorption/desorption envelopes of sulfate on goethite*

In this experiment, a pH envelope was produced by lowering the pH of the 0.01 M NaCl solution containing 20 μM SO_4 from 9.0 to 6.0 and then allowing the solution to reach steady state. The system was then lowered to pH 4.0 and equilibrated again. Next, the solution pH was raised back to 6.0 and then 9.0. At each step, the system was allowed to equilibrate until no changes in successive spectra occurred over a 15 min time. The results are shown in Fig. 5. From this figure, it can clearly be observed that more sulfate remains complexed on the goethite surface in the desorption samples than in the initial adsorption samples. It is important to note that potentiometric titrations (under N_2 atmosphere) of the goethite used in this study (data not shown) were fully and rapidly reversible. If hydrogen bonding is the dominant cause for the observed splitting of the sulfate bands, then one would expect that the desorption spectrum would very closely match the adsorption spectrum collected the same pH. However, in our experiment there is a general enhancement in the overall amount of sulfate adsorbed (higher absorbance in the desorption samples). This can be seen specifically in the 1170, 1132, and 1050 cm^{-1} peaks which are relatively larger in the desorption spectra than in the adsorption envelope. This is consistent with an inner-sphere complexation mechanism. Based upon this experimental evidence of inner-sphere complexation and the successful ETLM modeling of

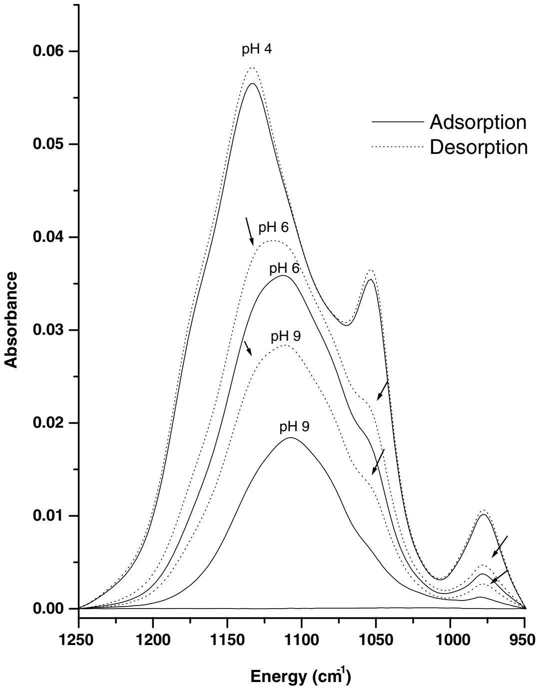

Fig. 5. Spectra from an adsorption/desorption envelope conducted with $I = 0.01$ M NaCl and $SO_4 = 25$ μM. Experiment was conducted by initially lowering the pH from 9.0 to 6.0 and then to 4.0 and collecting spectra at each pH. The pH was then returned to 6.0 and 9.0 and spectra were collected after desorption had reached steady state. Arrows denote spectral features indicative of inner-sphere complexes persisting after desorption had occurred.

Fukushi and Sverjensky (2007) using a monodentate inner-sphere plus an outer-sphere/hydrogen bonded complex, we will assign peaks at 1170, 1132, and 1050 cm^{-1} as arising from an inner-sphere species. There may be some additional hydrogen-bonding that occurs in the system, but it remains unknown whether those peaks would overlap with only the inner-sphere peaks, only the outer-sphere peaks, or with both complexes.

3.2.2. *Adsorption isotherm of sulfate on goethite*

The spectra of adsorption isotherm of sulfate at pH 4, 5, and 6 indicated that intensities of absorbance and peak positions of spectra obtained from ATR-FTIR depend upon both sulfate concentration and solution pH (Fig. 6). In all cases, the increased absorbance as concentration increases are due to increased sulfate loading, as is expected with an increase in aqueous sulfate concentrations. It was also clear from intensity of absorbance that less sulfate adsorption occurs as pH decreases. It is also worth noting that in all cases the absorbance of adsorbed sulfate is calculated to be responsible for over 99% of the total FTIR signal as free aqueous sulfate peak intensity is negligible below 250 μM SO_4.

At pH 4.0, there are multiple peaks present in all samples indicative of inner-sphere complexation of sulfate on goethite: ν_3 band splitting in the 1050–1200 cm^{-1} region and an IR active ν_1 band at 978 cm^{-1} (Fig. 6a). For the asymmetric stretch (ν_3) peaks at 1055, 1134 cm^{-1}, and a shoulder at 1170 cm^{-1} are all visible in the raw data, but become even more easily assignable in the difference spectra (Fig. 6d). These peaks become sharper and much well resolved with increasing sulfate concentrations, which implies that the relative amount of inner-sphere complexation increases with loading. However, it was not possible to fit any of the pH 4 experimental spectra without including a large broad gaussian peak at 1110 cm^{-1} arising due to outer-sphere sulfate.

On goethite at pH 5, the peaks in the raw spectra are not as well-resolved and the amount of splitting in the 1200–1050 cm^{-1} range is diminished compared to the pH 4.0 experiments. This can be explained by the fact that both outer-sphere and inner-sphere surface complexes are present, with relatively less inner-sphere adsorption occurring at pH 5 than at pH 4. Additionally, the results of raw spectra and difference spectra at pH 5 (Fig. 6b and e) clearly show that increasing the sulfate equilibrium concentrations do have an effect on the contribution of inner- and outer-sphere surface complexes to additional sulfate adsorption on goethite. At lower sulfate C_{eq} (5 μM), inner-sphere complex peaks are weakly visible, but as sulfate C_{eq} increases from 5 to 250 μM, three peaks at 978, 1055, and 1114–1128 cm^{-1} become sharper, and a weakly visible shoulder at 1170 cm^{-1} is present. These results suggest that the additional adsorption of sulfate as C_{eq} increases is, in large extent, due to inner-sphere complexes.

At pH 6.0, the isotherms are dominated by one large broad peak (ν_3) at approximately 1110 cm^{-1} that shifts slightly to higher wave number (1113 cm^{-1}) as sulfate C_{eq} is increased. A weakly IR-active ν_1 peak at 978 cm^{-1} was also present (Fig. 6c). These two observed features are consistent with an outer-sphere complex that generally retains its T_d symmetry. Some distortions from a purely tetrahedral molecule are expected since the interaction is electrostatic in nature (the goethite surface is positively-charged below pH 8.4). At higher concentrations, a shoulder at 1050 cm^{-1} was present in the raw data as well, and difference spectrum revealed that the highest concentration at pH 6 (250–100 μM) appears very similar to the lowest concentration difference spectrum at pH 5 (10–5 μM) (Fig. 6f). This is consistent with a small amount of inner-sphere complexation occurring at pH 6.0 at higher concentrations. However, outer-sphere complexation was the dominant complex formed at pH 6.

In summary, outer- and inner-sphere sulfate complexes occurred simultaneously in binary goethite/sulfate system under conditions of 5–250 μM sulfate C_{eq} and at pH 4, 5 and 6. Additional adsorption of inner-sphere sulfate complexes appeared more with increases of sulfate loading and lower pH values. These results are consistent with previous ATR-FTIR studies of sulfate on goethite (Peak et al., 1999, 2001; Elzinga et al., 2001), and provide a good baseline to compare the effects of Cd^{2+} on sulfate adsorption.

3.2.3. *Interaction of Cd and sulfate on goethite*

Fig. 7a and b show the spectra of 25 μM sulfate adsorption as function of added Cd at pH 5 and 6, respectively. Results from pH 4, were omitted because addition of Cd had a negligible effect upon sulfate adsorption on goethite.

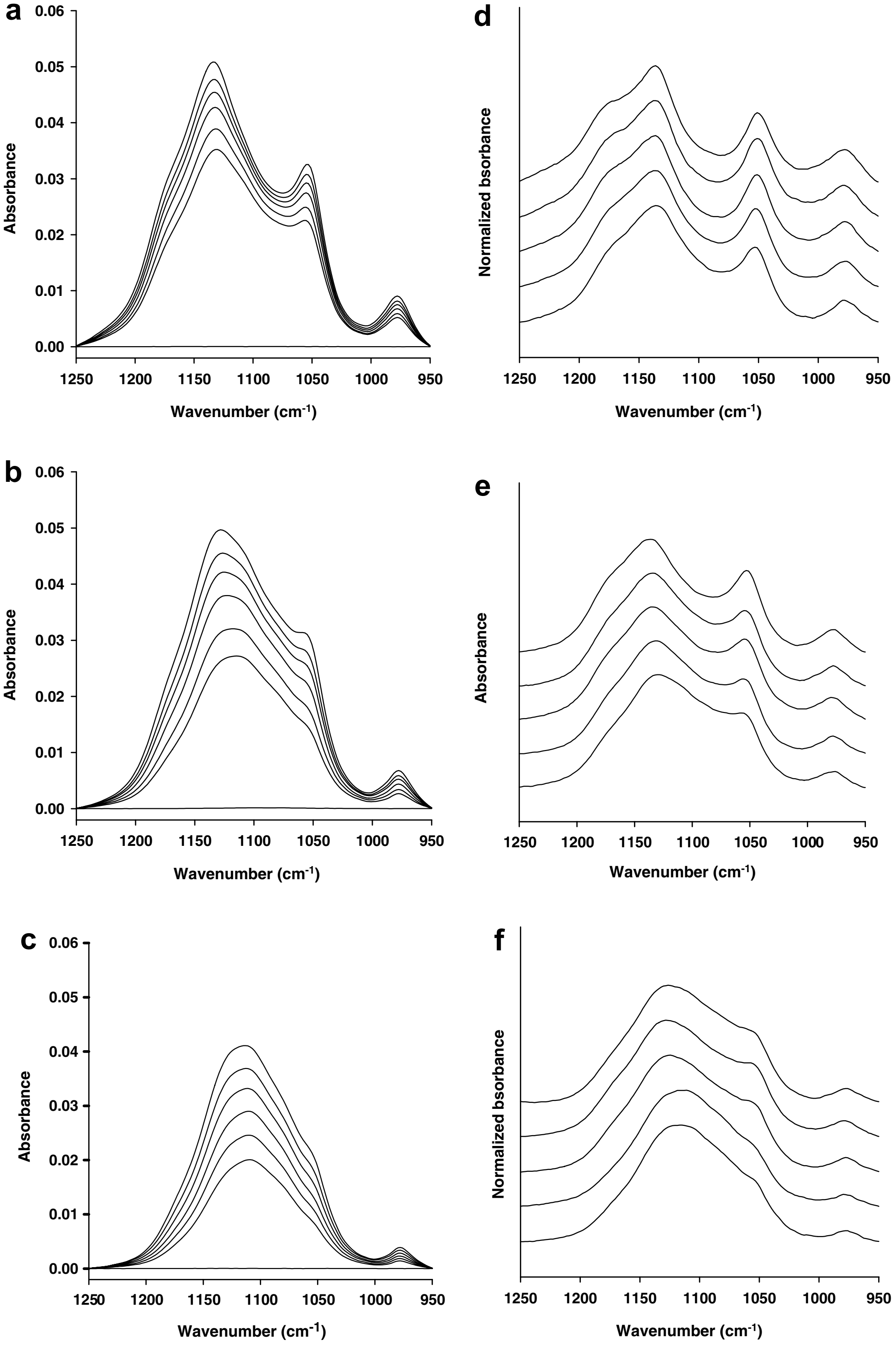

Fig. 6. Spectra from a sulfate adsorption isotherm conducted at (a) pH 4, (b) pH 5, (c) pH 6 and $I = 0.01$ M $NaNO_3$. The spectra are the results of (from bottom) 0, 5, 10, 25, 50, 100 and 250 μM equilibrium sulfate concentration. Difference spectra at (d) pH 4, (e) pH 5 and (f) pH 6 obtained from (a–c) by subtracting (from bottom) 5, 10, 25, 50 and 100 μM sulfate spectra from 10, 25, 50, 100 and 250 μM sulfate spectra, respectively.

At pH of 5 and 6, however, the IR absorbance of sulfate adsorption increased with rising Cd concentration from 10 to 500 μM. The effect of Cd addition was larger at pH 6 than at pH 5.

To clearly demonstrate the influence of introducing Cd on sulfate adsorption mechanisms, difference spectra were collected from raw spectra (Fig. 7c and d) by subtracting raw spectra of 25 μM sulfate adsorbed in the absence of Cd from adsorption spectra in the presence of 10, 25, 50, 100 and 500 μM Cd at pH 5 and 6, respectively. The resulting difference spectra (Fig. 7c and d) reveal the complexation mechanism of the additionally adsorbed sulfate.

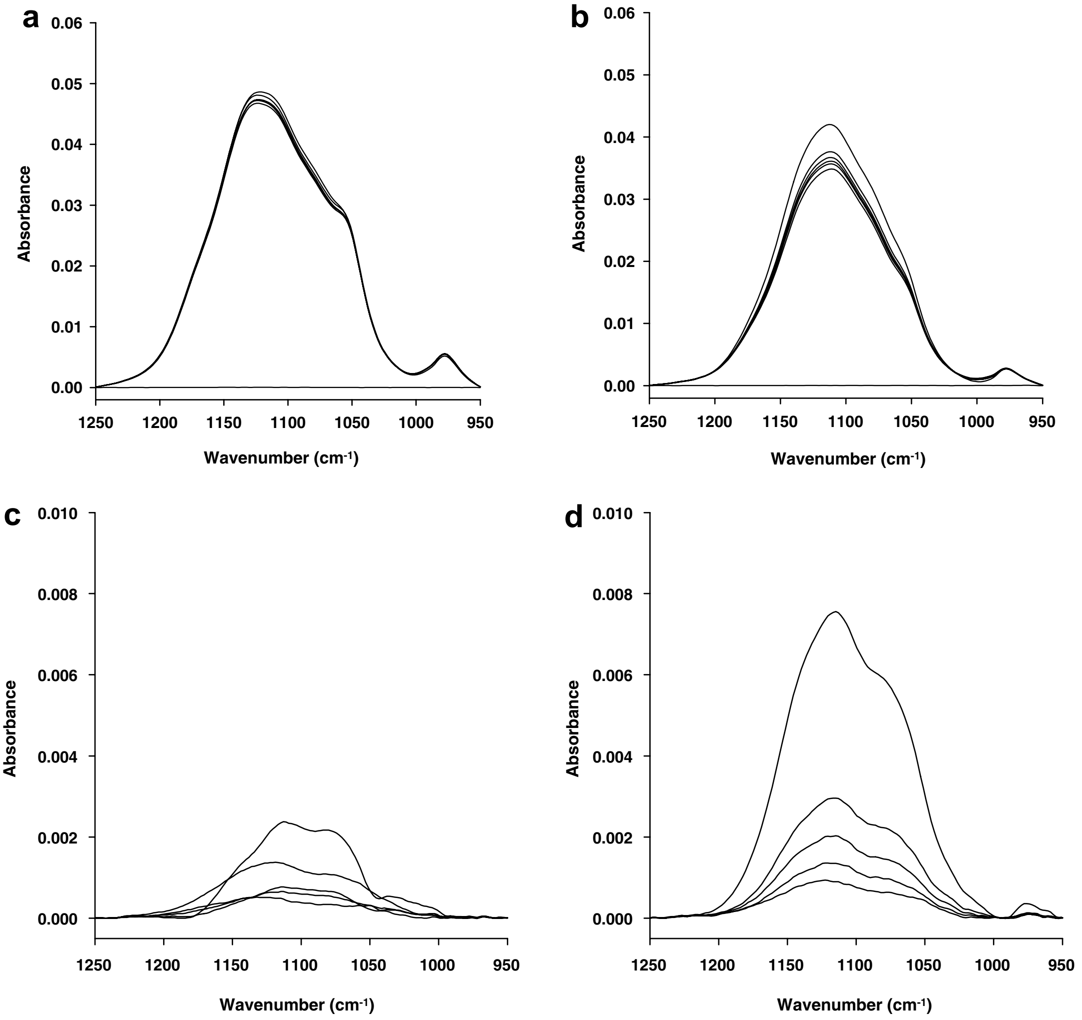

Fig. 7. Spectra of sulfate adsorption conducted as function of Cd at pH 5 (a) and pH 6 (b), respectively, in the conditions of $I = 0.01$ M $NaNO_3$ and $SO_4 = 25$ μM. The spectra are the results of (from bottom) 0, 5, 10, 25, 50, 100 and 500 μM equilibrium Cd concentration. Difference spectra of 25 μM SO_4 adsorption as function of Cd concentration at pH 5 (c) and pH 6 (d), from bottom they are 10–0, 25–0, 50–0, 100–0 and 500–0 μM Cd.

At both pH 5 and 6, increasing the Cd concentration resulted in the appearance of two peaks at approximately 1080 and 1115 cm^{-1} as well as a shoulder at ~1145 cm^{-1} in all difference spectra. The features become more obvious with increasing Cd concentration. This type of v_3 splitting was not observed in the spectra of sulfate adsorption on goethite in the absence of Cd, which is clear evidence that Cd addition caused the formation of an additional sulfate adsorption complex on goethite surface.

However, it is necessary to more carefully evaluate the shoulder at ~1145 cm^{-1}. In Fig. 8, a difference spectrum (500–0 μM Cd in 25 μM SO_4 at pH 5) at ~1145 cm^{-1} could indicate a change in symmetry previously observed in v_3 bands. Additionally, a feature (negative absorbance) at ~1050 cm^{-1} is present that corresponds well with one of the peak positions for inner-sphere sulfate adsorption on goethite. So it is possible that the appearance of shoulder at ~1145 cm^{-1} is actually caused by negative absorbance at ~1134 cm^{-1} which we would expect to accompany a negative absorbance at ~1050 cm^{-1} if a decrease of inner-sphere sulfate was responsible for the spectral features. The explanation is further supported by fact that no v_1 band is visible in difference spectrum of 500–0 μM Cd at pH 6. This can be explained by intensity of negative absorbance due to complex conversion being roughly equal to increases of absorbance from Cd addition. This strongly suggests that some of the inner-sphere sulfate complexes are either desorbing or converting to a different surface complex in the presence of Cd.

To eliminate any possible surface loading effects from the comparisons, difference spectra of sulfate isotherm (in free-Cd system) and sulfate adsorption in Cd-added system with similar absorbance intensities were compared. At pH 6.0, raising the SO_4 concentration from 25 to 100 μM in Cd-free systems leads to a similar increase in SO_4 adsorption as does raising the Cd concentration from 0 to 500 μM in the presence of 25 μM SO_4. At pH 5.0, the difference spectra obtained by raising the sulfate concentration from 25 to 50 μM is of comparable intensity as raising the Cd solution from 0 to 500 μM at 25 μM SO_4. Fig. 8

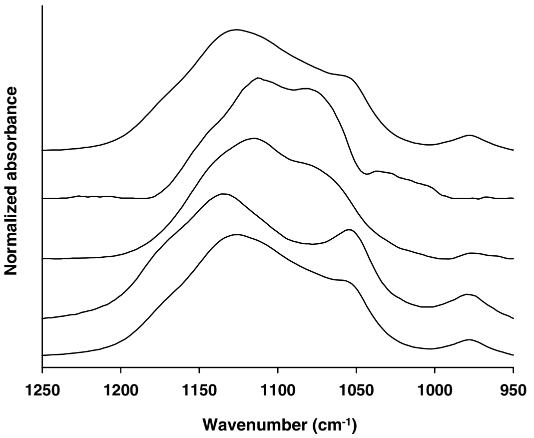

Fig. 8. Difference spectra between the SO_4 spectra obtained at 500 and 0 μM Cd concentration at pH 6 and 5, compared with difference spectra of inner-sphere sulfate complexes on goethite. From bottom: 100–25 μM SO_4 at pH 6, 50–25 μM SO_4 at pH 5; 500–0 μM Cd in 25 μM SO_4 at pH 6 and 5, respectively; 25 μM SO_4 at pH 4. All spectra were normalized to a maximum absorbance of 1 and then offset for comparison, so the absorbance values in this figure are arbitrary.

compares these four difference spectra as well as the spectrum of sulfate sorbed on goethite at pH 4. At pH 4, the spectral features of inner-sphere SO_4 complexes at the goethite surface are well resolved.

One can conclude from Fig. 8 that the additional sulfate complexation as a result of increasing Cd concentration was not simply due to increased sulfate surface loading. This is because the frequencies at ~1115 and ~1080 cm^{-1} did not appear in the difference spectra obtained from increasing the SO_4 solution concentrations in Cd-free systems (Fig. 8). Comparison with the spectrum of SO_4 sorbed on goethite at pH 4 illustrate that the peak positions and number of peaks of ν_3 splitting are different between the inner-sphere SO_4 complexes in the absence and presence of Cd. In the absence of Cd, the ν_3 band split into two peaks centered at 1055, 1132 cm^{-1} and a shoulder at 1170 cm^{-1}, whereas in the presence of Cd at pH 5 or pH 6, ν_3 band was split into two frequencies located at ~1115 and ~1080 cm^{-1}. Therefore, the appearance of frequencies ~1115 and ~1080 cm^{-1} with Cd present are consistent with SO_4 present in a new ternary complex with monodentate-like symmetry (C_{3v}).

4. DISCUSSION

ATR-FTIR data indicated that Cd–SO_4 ternary complexes form at the goethite surface, especially at high Cd concentration. The sulfate ions in these complexes have C_{3v} symmetry with relatively weak splitting. Based on the results that Cd sorbed in the mode of bidentate binuclear on goethite in the range of pH 4 to 5.9 (Collins et al., 1999; Randall et al., 1999; Boily et al., 2005), our conclusion from the adsorption/desorption envelope that inner-sphere complexes are responsible for the splitting, and consideration of IR spectra observed in this study, potential configurations of Cd–SO_4 ternary complexes consistent with previous Cd EXAFS results of other

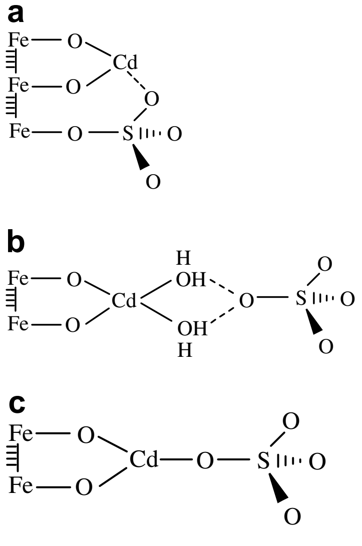

Fig. 9. Cd–SO_4–goethite ternary complex configurations consistent with the FTIR data. The labels a–c denote different bonding mechanisms that are discussed in detail in the text.

researchers and our current ATR-FTIR study were assumed as Fig. 9.

For evaluation of which complexes are most likely to form, more information of how Cd–SO_4 interactions affect the IR spectra of standard compounds is necessary. Several relevant FTIR reference spectra were collected and are shown in Fig. 10. The SO_4^{2-} spectrum is dominated by a single broad peak centered at 1102 cm^{-1}. This is the asymmetric stretch (ν_3) band of sulfate in a purely tetrahedral (T_d) configuration. The $HSO_{4(aq)}^{-1}$ spectrum actually contains some SO_4^{2-} as well (the peak at 1105 cm^{-1}) due to the sample's pH, but also shows strong splitting of the υ_3 band at 1197 and 1053 cm^{-1} which indicates a C_{3v} bonding environment. The degree of splitting (~144 cm^{-1}) is consistent with strong covalent bonding between H^+ and SO_4^{2-}. The spectrum of $CdSO_{4(aq)}^0$ ion pair is close to that of SO_4 (Na_2SO_4) in aqueous solution, which indicate that T_d

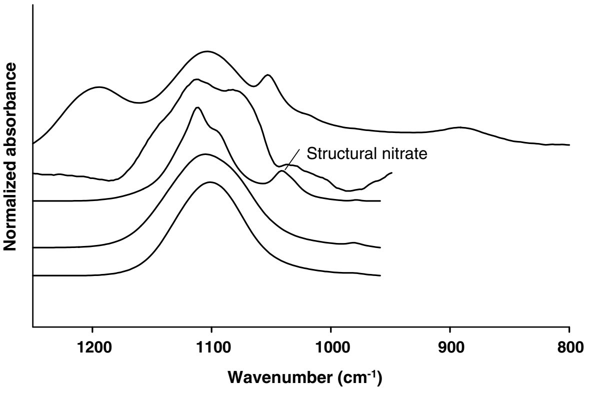

Fig. 10. Comparison of the pH 5 difference spectrum and standards. From bottom: $SO_{4(aq)}$, $CdSO_{4(aq)}$, $CdSO_4{\cdot}OH_{(s)}$, 500–0 μM Cd at pH 5 and HSO_4^-. All spectra were normalized to a maximum absorbance of 1 and then offset for comparison, so the absorbance values in this figure are arbitrary.

symmetry is largely retained. However, its v_1 band is slightly active, and v_3 band shows a slight shift toward higher wavenumbers relative to the spectrum of $SO_{4(aq)}$.It is possible that slight splitting of the v_3 band is responsible for the broadening of the peak. This is consistent with $CdSO_{4(aq)}{}^0$ complexation in solution being mainly due to electrostatic interactions, which lead to small distortions of the SO_4 tetrahedron.

If it is assumed that Cd–SO_4 bonding at the goethite surface is also mostly electrostatic, then configuration A (Fig. 9) would be the most reasonable structure for the Cd–SO_4 ternary complexes forming at the goethite surface. This structure can be considered as analogous to the inner-sphere SO_4 configurations forming on goethite as proposed by Peak et al. (1999, 2001). They suggested the inner-sphere sulfate complex was a monodentate sulfate surface complex with additional hydrogen bonding to an adjacent goethite surface site. In configuration A, SO_4 forms a monodentate inner-sphere complex with the FeOOH surface and there is some additional interaction with an adjacent adsorbed Cd metal ion. How this would be expected to affect the spectrum are dependent upon the strength of the interactions between the SO_4 oxygen and Cd. If Cd–O bond ≪ H–O bond in strength, then configuration A would show C_{3v}-like symmetry of SO_4. If Cd–O bond is roughly equal to H–O bond in strength, the spectrum would be C_s/C_1 symmetry and similar in appearance to SO_4 on goethite without Cd present. From the aqueous standards it is clear Cd–SO_4 produces weaker v_3 splitting than does $HSO_4{}^-$. Replacing the strong H–SO_4 interaction with a relatively weak Cd–SO_4 bond, as shown in configuration A would therefore be expected to lead to less-distorted SO_4 tetrahedron with monodentate-like (C_{3v}) symmetry. This is consistent with the observed number of peaks in the Cd–SO_4 ternary complexes, but not with the peak positions. If the Cd–SO_4 interaction is weak then the monodentate surface complex should appear virtually identical to sulfate adsorbed on hematite via a monodentate inner-sphere mechanism (Hug, 1997). In this bonding environment, the v_3 peaks are present at 1122 and 1060 cm^{-1} which is not consistent with the observed ternary complex features.

In configuration B (Fig. 9), Cd is again coordinated in bidentate binuclear fashion to goethite surface as suggested by the EXAFS results of other researchers (Collins et al., 1999). In this complex, sulfate is electrostatically interacting with the adsorbed Cd in outer-sphere complexes. By itself, such an interaction would produce a T_d-distorted symmetry, not C_{3v} symmetry. However, additional hydrogen bonding to functional groups or surface waters plus the electrostatic attraction could theoretically lead to C_{3v}-like symmetry of SO_4 observed in the ternary complex. If the Cd–SO_4 ternary complex is coordinated with an inner-sphere monodentate bonding instead of an outer-sphere coordination, then formation of configuration C (Fig. 8) would occur. Therefore, both B and C are reasonable based upon symmetry arguments alone. To determine the expected positions of vibrations in inner-sphere Cd–SO_4 complexes, the spectrum of a cadmium sulfate precipitate was collected. One can clearly see that the spectrum of $CdSO_{4(s)}$ has sharp peaks at 1111, 1095 cm^{-1} and weakly visible peak at 978 cm^{-1} (Fig. 10). This is fairly good agreement with our observed ternary complex peak positions. Therefore, we conclude that configuration C is consistent with the observed experimental spectra.

The presence of Cd also has some indirect effects on the complexation mechanisms of sulfate. For example, at pH 5 the difference spectrum of 500–0 μM Cd (Fig. 8) shows negative absorbance at ~1055, ~1134 and ~1175 cm^{-1}, which are the v_3 band locations of inner-sphere sulfate complexes forming in Cd-free system. The negative absorbance indicates that a fraction of inner-sphere sulfate complexes are being replaced or transformed into Cd–SO_4 ternary complexes in the condition of 500 μM Cd at pH 5. At pH 6, not all of the increased absorbance in the presence of Cd can be attributed to increased absorbance in the ternary complex region. Additional outer-sphere and inner-sphere adsorption of sulfate must also be partially responsible.

There is also an effect of increased Cd concentration on SO_4 adsorption mechanisms. This can be directly observed by sequentially subtracting spectra sulfate adsorbed in the presence of lower Cd concentration from higher concentration Fig. 11 shows the results of this experiment at pH 6.0. The results illustrate several points: (1) The frequencies arising from Cd–SO_4 ternary complexes are more obvious for the difference spectra at higher Cd concentrations, (2) Cd concentration from 25 to 500 μM leads to negative absorbance at the spectral locations of the v_3 bands (1050–1200 cm^{-1}) of the inner-sphere SO_4 complex that ccurs in Cd-free system, (3) The relatively broad peak of 10–0 μM Cd indicate that additional SO_4 adsorption occurs not only due to formation of Cd–SO_4 ternary complexes but also additional inner- and outer-sphere SO_4 complexation. In Fig. 8, negative absorption is observed for difference spectrum of 500–0 μM Cd at pH 5 and 6. Those observations above imply transformation of C_s symmetry of inner-sphere SO_4 complex into Cd–SO_4 ternary complex upon addition of Cd.

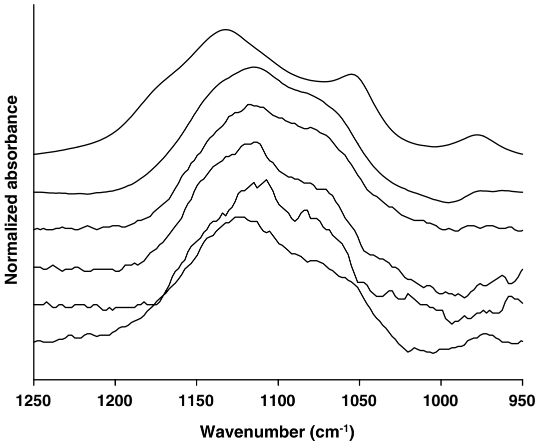

Fig. 11. Difference spectra of SO_4 adsorption as function of Cd concentration at pH 6. The difference spectra are collected (from bottom) by subtracting 0, 10, 25, 50 and 100 μM Cd spectra from 10, 25, 50, 100, and 500 μM Cd spectra, respectively; the top spectrum is 25 μM SO_4 at pH 4. All spectra were normalized to a maximum absorbance of 1 and then offset for comparison, so the absorbance values in this figure are arbitrary.

A comparison of the difference spectrum of 500–0 μM at pH 5 with that of pH 6 reveals that relatively more SO_4 outer-sphere complexes occur with Cd addition at pH 6. As described previously, although ternary complex formation is observed at both pH values, it seems to be especially important at pH 5.0. At a fixed pH value, SO_4 adsorption by ternary complex formation becomes more important with increasing Cd concentration. Moreover, a portion of the SO_4 initially sorbed in inner-sphere complexes on goethite is transformed into Cd–SO_4 ternary complex with rising Cd concentration.

Adsorption of Cd on goethite also affects SO_4 adsorption by surface charge effects. It was reported that Cd binds to goethite as inner-sphere complexes (Collins et al., 1999), which will create additional positive surface charge and result in more favorable conditions for SO_4 adsorption. Cd adsorption is enhanced by higher pH (Fig. 4), which explains the relatively strong electrostatic effect on sulfate adsorption at pH 6. These results imply that pH value does not only affect the extent of adsorption, but also the mechanisms of additional SO_4 adsorption. At lower pH (pH 5), additional SO_4 complexes occurs to a large extent via inner-sphere complexation, whereas at pH 6.0 a relatively large fraction adsorbs via outer-sphere complexation. Low pH values and high Cd concentration promoted transformation of inner-sphere SO_4 complexes into Cd–SO_4 ternary complexes.

There are some differences in both peak positions and number of peaks between Cd–SO_4 ternary complexes observed in this study and the Pb–SO_4 ternary complexes sorbed on goethite from previous research. Elzinga et al. (2001) reported two dominant peaks of sulfate adsorption on goethite at 1110 and 1070 cm^{-1} at pH 4.5–6.0 in 1 mM Pb and 30 μM sulfate system. In contrast, Ostergren and co-workers (2000) observed that Pb–SO_4 ternary complexation on goethite produced two dominant bands of near 1150 and 1050 cm^{-1}, and a relatively weak peak at ~1100 cm^{-1} with 0.1 mM Pb and 631 μM SO_4 at pH 5. The spectra of Cd–SO_4–goethite ternary complex observed in this experiment appeared two peaks at ~1115 and ~1080 cm^{-1}, which are fairly consistent with Elzinga and co-workers results. The difference in peak positions is likely related to following factors: (1) Variations of chemical properties of Pb and Cd, such as hydrolysis constants (pK_a): Pb 7.7 > Cd 10.1, and electronegativity Pb: 1.7 > Cd 1.6. (2) The solubility of $PbSO_4$ is far lower than $CdSO_4$. (3) Experiments were conducted in very different conditions (pH, metal concentration, and sulfate concentration) by some other researchers.

ACKNOWLEDGMENTS

Senior author thanks China Scholarship Council for financial support. This research is partially supported by National Science and Engineering Research Council of Canada (NSERC). Help from D. Xu and P.G. Burnett is greatly appreciated.

REFERENCES

Ali M. A., and Dzombak D. A. (1996) Interactions of copper, organic acids, and sulfate in goethite suspensions. *Geochim. Cosmochim. Acta* **60**, 5045–5053.

Bargar J. R., Brown, Jr., G. E., and Parks G. A. (1998) Surface complexation of Pb(II) at oxide–water interfaces. III. XAFS determination of Pb(II) and Pb(II)-chloro adsorption on goethite and alumina. *Geochim. Cosmochim. Acta* **62**, 193–207.

Benjamin M. M., and Leckie J. O. (1982) Effects of complexation by Cl, SO_4, and S_2O_3 on adsorption behavior of Cd on oxide surfaces. *Environ. Sci. Technol.* **16**, 162–170.

Boily J. F., Sjoberg S., and Persson P. (2005) Structures and stabilities of Cd(II) and Cd(II)–phthalate complexes at the goethite/water interface. *Geochim. Cosmochim. Acta* **69**(13), 3219–3235.

Collins C. R., Ragnarsdottir K. V., and Sherman D. M. (1999) Effect of inorganic and organic ligands on the mechanism of cadmium sorption to goethite. *Geochim. Cosmochim. Acta* **63**, 2989–3002.

Coughlin B. R., and Stone A. T. (1995) Nonreversible adsorption of divalent metal ions (MnII, CoII, NiII, CuII, and PbII) onto goethite: effects of acidification, FeII addition, and picolinic acid addition. *Environ. Sci. Technol.* **29**, 2445–2455.

Davis A. P., and Bhatnagar V. (1995) Adsorption of cadmium and humic acid onto hematite. *Chemosphere* **30**, 243–256.

Elzinga E. J., Peak D., and Sparks D. L. (2001) Spectroscopic studies of Pb(II)-sulfate interactions at the goethite–water interface. *Geochim. Cosmochim. Acta* **65**(14), 2219–2223.

Fukushi K., and Sverjensky D. A. (2007) A surface complexation model for sulfate and selenate on iron oxides consistent with spectroscopic and theoretical molecular evidence. *Geochim. Cosmochim. Acta* **71**(1), 1–24.

Hind A. R., Bhargava S. K., and McKinnon A. (2001) At the solid/liquid interface: FTIR/ATR—the tool of choice. *Adv. Colloid Interface Sci.* **93**, 91–114.

Hoins U., Charlet L., and Sticher H. (1993) Ligand effect on the adsorption of heavy metals: the sulfate–cadmium–goethite case. *Water Air Soil Poll.* **68**, 241–255.

Hug S. J. (1997) In situ Fourier transform infrared measurements of sulfate adsorption on hematite in aqueous solutions. *J. Colloid Interface Sci.* **188**, 415–422.

Lackovic K., Angove M. J., Wells J. D., and Johnson B. B. (2004) Modeling the adsorption of Cd(II) onto goethite in the presence of citric acid. *J. Colloid Interface Sci.* **269**(1), 37–45.

Lamy I., Djafer M., and Terce M. (1991) Influence of oxalic acid on the adsorption of cadmium at the goethite surface. *Water Air Soil Poll.* **57–58**, 457–465.

Lefevre G. (2004) In situ Fourier-transform infrared spectroscopy studies of inorganic ions adsorption on metal oxides and hydroxides. *Adv. Colloid Interface Sci.* **107**, 109–123.

Marcano-Martinez E., and McBride M. B. (1989) Calcium and sulfate retention by two oxisols of the Brazilian Cerrado. *Soil Sci. Soc. Am. J.* **53**, 63–69.

Majzlan J., and Myneni S. C. B. (2005) Speciation of iron and sulfate in acid waters: aqueous clusters to mineral precipitates. *Environ. Sci. Technol.* **39**(1), 188–194.

Nowak B., and Sigg L. (1996) Adsorption of EDTA and metal–EDTA complexes onto goethite. *J. Colloid Interf. Sci.* **177**, 106–121.

Ostergren J. D., Brown G. E., Parks G. A., and Persson P. (2000) Inorganic ligand effects on Pb(II) sorption to goethite (a-FeOOH). II. Sulfate. *J. Colloid Interface Sci.* **225**, 483–493.

Peak D., Elzinga E. J., and Sparks D. L. (2001) Understanding sulfate adsorption mechanisms on iron (III) oxides and hydroxides: results from ATR-FTIR spectroscopy. In: *Heavy Metals Release in Soils* (eds. H. Magdi Selim, and Donald L. Sparks). CRC Press LLC, Boca Raton London, New York, Washington, DC, pp. 167–190.

Peak D., Ford R. G., and Sparks D. L. (1999) An in situ ATR-FTIR investigation of sulfate bonding mechanisms on goethite. *J. Colloid Interface Sci* **218**, 289–299.

Peak J. D., and Sparks D. L. (2002) Mechanisms of selenate adsorption on iron oxides and hydroxides. *Environ. Sci. Technol.* **36**, 1460–1466.

Persson P., and Lovgren L. (1996) Potentiometric and spectroscopic studies of sulfate complexation at the goethite–water interface. *Geochim. Cosmochim. Acta* **60**, 2789–2799.

Randall S., Sherman D. M., and Ragnarsdottir K. V. (1999) The mechanism of cadmium adsorption to iron oxyhydroxides. *Geochim. Cosmochim. Acta* **63**(19/20), 2971–298.

Schwertmann U., Cambier P., and Murad E. (1985) Properties of goethites of varying. *Clays Clay Miner.* **33**, 369–378.

Swedlund P. J., Webstera J. G., and Miskelly G. M. (2003) The effect of SO_4 on the ferrihydrite adsorption of Co, Pb and Cd: ternary complexes and site heterogeneity. *Appl. Geochem.* **18**, 1671–1689.

Theis T. L., and West M. J. (1986) Effects of cyanide complexation on adsorption of trace metals at the surface of goethite. *Environ. Technol. Lett.* **7**, 309–318.

Webster J. G., Swedlund P. J., and Webster K. S. (1998) Trace metal adsorption onto an acid mine drainage iron(III) oxy hydroxy sulfate. *Environ. Sci. Technol.* **32**, 1361–1368.

Associate editor: Dimitri A. Sverjensky